Journal of Crohn's and Colitis, 2025, **19(10)**, jjaf180
https://doi.org/10.1093/ecco-jcc/jjaf180
Advance access publication 15 October 2025
Original Article

Spatial transcriptomics reveals unique inflammatory signatures across all anatomic locations in postoperative Crohn's disease

Robert Battat*[1,2], Bruno Sangiorgi[3], Bryan Linggi[3], Xianyong Gui[4,5], Michelle I. Smith[3], Saurabh Mehandru[6], Randy Longman[2], Dana J. Lukin[2], Ellen J. Scherl[2], Lihui Qin[7], Christopher Ma[3,8,9], Wendy Teft[3], Niels Vande Casteele*[4,10]

[1]Division of Gastroenterology and Hepatology, University of Montreal Hospital Center, Montreal, QC, Canada
[2]Division of Gastroenterology and Hepatology, Weill Cornell Medicine, Jill Roberts Center for IBD, New York, NY, United States
[3]Alimentiv Inc, London, ON, Canada
[4]AcelaBio Inc, San Diego, CA, United States
[5]Department of Pathology, Wake Forest University School of Medicine, Winston-Salem, NC, United States
[6]Department of Medicine, Division of Gastroenterology, Icahn School of Medicine at Mount Sinai, New York, NY, United States
[7]Department of Pathology and Laboratory Medicine, Division of Anatomic Pathology, New York-Presbyterian Hospital, Weill Cornell Medical College of Cornell University, New York, NY, United States
[8]Division of Gastroenterology & Hepatology, Cumming School of Medicine, University of Calgary, Calgary, AB, Canada
[9]Department of Community Health Sciences, Cumming School of Medicine, University of Calgary, Calgary, AB, Canada
[10]Department of Medicine, University of California San Diego, San Diego, CA, United States

*Corresponding authors: Niels Vande Casteele, Department of Medicine, University of California, San Diego, 9500 Gilman Drive #0956, La Jolla, CA 92093, United States (nvandecasteele@ucsd.edu) and Robert Battat, Center for Clinical Excellence and Translational Research in Inflammatory Bowel Diseases, Centre Hospitalier de l'Université de Montréal, 900 Saint Denis St, Montreal, Quebec H2X 0A9, R08.430, Canada (robert.battat@umontreal.ca).

Robert Battat and Bruno Sangiorgi contributed equally to this work as first authors.

Conference presentation: This work was previously presented at the 19th Congress of the European Crohn's and Colitis Organisation (February 21-24, 2024; Stockholm, Sweden), Digestive Disease Week (May 18-21, 2024; Washington, DC, United States), and at the 3rd Annual Precision Medicine in Inflammatory Bowel Disease Summit (May 13-15, 2025; Boston, MA, United States).

Abstract

Background and Aims: Most patients with Crohn's disease (CD) who have undergone ileocolonic resection experience recurrent inflammation within 1 year after surgery. We examined the molecular basis underlying gastrointestinal inflammation in postoperative CD across 3 common anatomic locations of recurrence.

Methods: To characterize spatial transcriptomic signatures, this study utilized biopsies from the colon, neo-terminal ileum, and anastomosis of patients with postoperative CD in the PREDICT-OR study. Sample analyses were performed with 10X Genomics Visium CytAssist system V2.0, and data analyses with R.

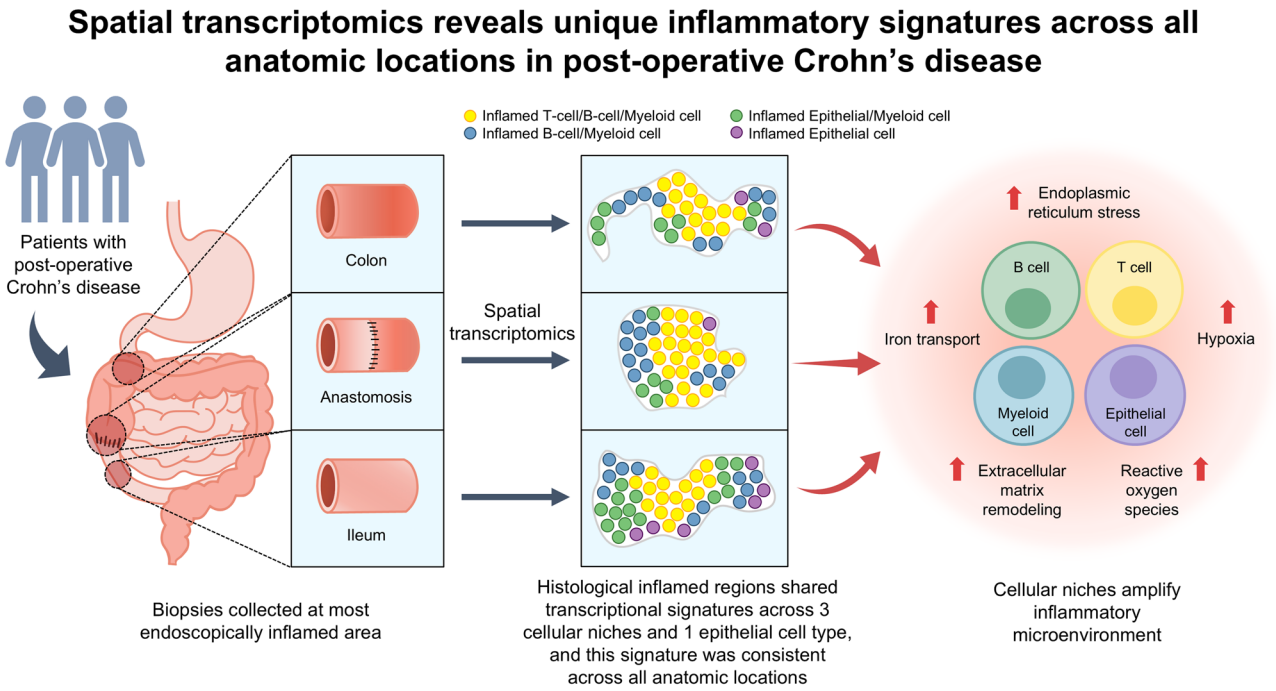
Results: Histologically inflamed biopsies from all locations shared transcriptional signatures across 3 cellular niches (myeloid, B, T cells) and a specialized epithelial cell type expressing inflammation-associated genes. Differentially expressed genes overexpressed inflammatory pathway activity across the 3 locations, whereas hypoxic pathways were less apparent. In addition to genes for known treatment targets, epidermal growth factor receptor and mitogen-activated protein kinase pathways were upregulated. Cellular niches shaped inflammatory microenvironments through endoplasmic reticulum stress and extracellular matrix remodeling signaling.

Conclusions: Application of spatial transcriptomics revealed a common disease signature for postoperative CD across the colon, neo-terminal ileum, and anastomosis. Inflamed biopsies from all locations demonstrated similar immune cell and inflammatory gene expression patterns as opposed to hypoxic pathways, and unique inflammatory pathways were revealed.

Key words: molecular pathology; RNA expression; histopathology.

© The Author(s) 2025. Published by Oxford University Press on behalf of European Crohn's and Colitis Organisation.
This is an Open Access article distributed under the terms of the Creative Commons Attribution-NonCommercial License (https://creativecommons.org/licenses/by-nc/4.0/), which permits non-commercial re-use, distribution, and reproduction in any medium, provided the original work is properly cited. For commercial re-use, please contact reprints@oup.com for reprints and translation rights for reprints. All other permissions can be obtained through our RightsLink service via the Permissions link on the article page on our site—for further information please contact journals.permissions@oup.com.

Graphical abstract



1. Introduction

Most patients with Crohn's disease (CD) require ileocolonic resections, and intestinal inflammation recurs in up to 70% of patients within 1 year after surgery.[1] This recurrence is associated with complications including corticosteroid use, hospitalization, reoperation,[2–5] and increased morbidity.[6] There is an unmet medical need for effective treatments of recurrent CD after ileocolonic resection. The current lack of therapeutic options in postoperative CD is partially attributable to a limited understanding of its molecular basis, uncertainties about the relative contributions of ischemia and inflammation to the development of anastomotic ulcers,[7] and conflicting reports of the relationships between CD location, postsurgical outcomes, and disease recurrence.[7,8]

Spatial transcriptomics has advanced the ability to identify previously hidden signals in inflammatory bowel disease (IBD). This method avoids noise cancellation caused by (1) a lack of cellular information (next-generation sequencing) or (2) a lack of spatial context (single-cell ribonucleic acid [RNA] sequencing). Increasing the resolution from bulk to single-cell RNA-sequencing identifies diverse cell populations, including immunoglobulin G plasma cells, myeloid cells, T cells, and mesenchymal cells, that mediate resistance to anti-tumor necrosis factor (TNF) therapy in CD.[9] However, similar cells in different locations can exist, and these signals can be lost without stratifying for spatial location. Spatial transcriptomics has provided comprehensive cellular and molecular characterizations of diseases with histologic and architectural context (ie, spatial maps of cellular niches within tissues) and insights into molecular interactions with neighboring cells.[10] However, a spatial transcriptomic signature of CD has not yet been elucidated.

This study utilized spatial transcriptomic analyses from mucosal biopsies across 3 anatomic locations to identify the spatial transcriptomic signature in postoperative CD.

2. Materials and methods

2.1 Biopsy procurement

Biopsies were from the Pharmacokinetic and Pharmacodynamics of Therapies, Noninflammatory Surgical Complications and Predictive Biomarkers in Postoperative Crohn's Disease (PREDICT-OR) study, which was approved by the Weill Cornell Medical College Institutional Review Board (#00009417, #00009419; ID 19-09020855), and all patients provided prior consent to participate. Biopsies were collected at the most endoscopically inflamed area in each location or at 5-10 cm from the anastomosis when no endoscopic inflammation was evident in the neo-terminal ileum or colon by postoperative ileocolonoscopy. All biopsies were fixed in 10% formalin and processed for routine paraffin embedding (Figure 1).

2.2 Tissue preparation and spatial transcriptomics

Total RNA was extracted from each formalin-fixed paraffin-embedded (FFPE) tissue block using the FormaPure XL RNA Reagent Kit and assessed for quality (PN C36001, Beckman Coulter). Only FFPE tissue blocks containing RNA of sufficient quality (DV_{200} ≥30%, indicating that ≥30% of the extracted RNA transcripts were at least 200 nucleotides in length) were used for subsequent analyses. Suitable FFPE tissue blocks were sectioned (4 µm, Histocore BIOCUT, Leica). Sections were placed on positively charged Superfrost Plus slides (catalogue no.1255015, Fisherbrand), heat-fixed in a section dryer oven (Epredia) at 60 °C for 30 minutes, deparaffinised, and stained with hematoxylin (catalogue no.7221, Epredia) and eosin (catalogue no.220-104, Epredia) (H&E) using a Histotek SL (Sakura) autostainer, and coverslipped. Whole slide images were acquired at ×40 magnification using an Aperio AT2 DX (Leica) high-precision scanner.

Spatial transcriptomic analyses were performed using the Visium 2.0 CytAssist system (10X Genomics).

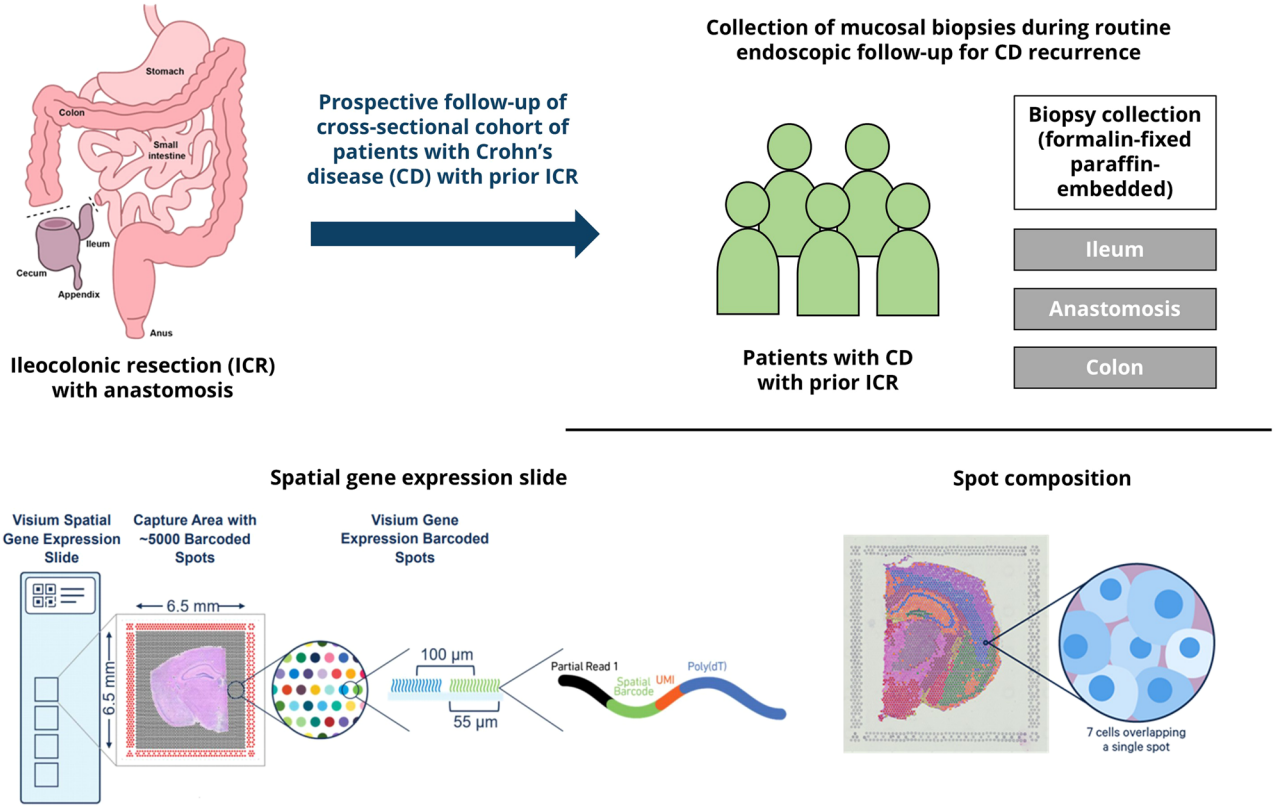


Figure 1. Methods overview.
Abbreviations: CD, Crohn's disease; ICR, ileocolonic resection.

2.3 Disease activity analyses used for spatial transcriptomic analyses

Transcriptomic pathway activity at the sample level was linked to histologic and endoscopic inflammation or a combination of both endoscopic and histologic inflammatory status (see "Disease activity assessments and definitions" section). Inflamed biopsy regions were compared to biopsy regions that were not inflamed and biopsy regions that were adjacent to inflamed biopsy regions. As histologic inflammation was the predominant determinant of pathway activity at the sample level, this definition was used to classify the cell populations according to associations with inflammation as well as transcriptomic pathway activity at the level of cell population.

2.4 Disease activity assessments and definitions

Whole slide images were assessed for histologic disease activity by a US Board–Certified gastrointestinal pathologist (X.G.) and scored using the Robarts Histopathology Index (RHI). Absence of histologic disease activity was defined as an RHI score of 3 or less, without neutrophil infiltration in the epithelium and lamina propria.[11] Postoperative disease recurrence was defined endoscopically as a Rutgeerts score of at least i2 or an SES-CD score of at least 3.

2.5 Alignment on Visium slides, histopathological annotations, and data export

After coverslip removal and destaining, the sections were processed for spatial transcriptomic analysis using the Visium 2.0 CytAssist system to position them over spots on Visium slides with a 6.5 mm^2 reaction area (1000519, 10x Genomics). Histopathological annotations of the whole slide images overlaying spots in the Visium slides (Figure 1) were provided for analyses (.cloupe files) by the study pathologist (X.G.) using Loupe Browser software (10x Genomics version 6.5.0). Spots overlaying areas of histologically inflamed biopsy regions were annotated as "inflamed," those overlayed with noninflamed areas of samples containing histologic inflammation were annotated as "adjacent-inflamed," while those overlayed with samples without evidence of histologic inflammation were annotated as "noninflamed." Spot-level histopathological annotations were exported into. csv files and loaded into the R environment for import into Seurat objects.

2.6 Sequencing library generation and genome alignment

The cDNA libraries were prepared from the sections according to Visium CytAssist Spatial Gene Expression for FFPE User Guide (CG000520 Rev B, 10x Genomics) and sequenced on an Illumina NovaSeq 6000 platform using version 1.5 reagent kits and NovaSeq Control Software version 1.7.5. Space ranger software (10x Genomics, version 2.0.0) was used for sequence alignment with the hg38 reference genome, tissue detection, fiducial detection, and barcode/unique molecular identifier (UMI) counting using whole slide images and sequencing (.fastq.gz) files as inputs. Output files included run summaries containing quality metrics, filtered feature-barcode matrices for spots overlayed with tissue sections, high-resolution images, and Loupe Browser files (.cloupe).

2.7 Data preprocessing

Feature barcode matrices, high-resolution images, and spot-image coordinates were imported into Seurat (version 4.4.0) objects, a data structure used for storing and manipulating

high-dimensional genomics data, including single-cell RNA sequencing and spatial transcriptomics.[12] Seurat objects corresponding to individual samples were merged into a single object using the "merge" function of the Seurat package. Based on the overall data distribution, spots without UMIs, more than 17% mitochondrial and/or hemoglobin gene transcripts, or less than 150 features were filtered out of the dataset. Spot-level histopathology annotations were imported using the "AddMetaData" function of the Seurat package, while sample-level metadata (eg, endoscopic inflammation, biopsy location, and histologic disease activity) were imported using base R (version 4.4.0) functions.

2.8 Batch correction, dimensional reduction, and trajectory analyses

Adjustments for the batch effects of multiple donors were achieved using the Harmony package.[13] Harmony reduction was used for uniform manifold approximation and projection (UMAP) dimensional reduction and the Nearest-neighbor graph construction via the "RunUMAP" and "FindNeighbors" Seurat functions, respectively, and by using the first 30 dimensions as input features. Clusters (or cell populations) were then identified using the "FindClusters" Seurat function with a resolution setting of 0.6.

Trajectory analyses were performed using the slingshot R package, which was designed to model developmental trajectories in single-cell RNA sequencing data.[14] The lines connecting developmental trajectories were manually overlayed with the UMAP plot data generated using the dittoSeq R package (version 1.16.0).

2.9 Cell type deconvolution

Spatial transcriptomic spots were deconvoluted using R package spacerx (version 2.2.1), following the guidelines for Robust Cell Type Decomposition (RCTD)[15] and the reference single-cell RNA-seq dataset from Elmentaite et al.[16] Prior to analysis, RNA transcripts derived from fetal and pediatric tissue were removed from the reference dataset to focus our analyses on adult human tissues. RCTD was subsequently performed in "full" mode, allowing for any number of cell types per spot, to accommodate the high resolution of 10X Visium Spatial Transcriptomics. Spots were assigned to an individual cell type based on the most predominant cell population within each spot. During downstream analysis, cell types contributing to less than 5% of the total composition of cell populations were filtered out of the dataset to capture and explore molecular signatures within cell populations representative of each population.

2.10 Ligand-receptor analysis

The R package NICHES (version 1.0.0) was used to analyse the local cellular microenvironment by analyzing transcripts encoding ligand-receptor pairs within spots in close-proximity.[17] This analysis was performed in accordance with the NICHES package vignette (https://msraredon.github.io/NICHES/articles/01%20NICHES%20Spatial.html) for estimating the microenvironment from spatial transcriptomic data. Briefly, the adaptively thresholded low-rank approximation (ALRA)[18] assay was performed with Seurat Wrappers (SeuratWrappers::RunALRA) and used for ligand-receptor pair analysis with the ligand-receptor database FANTOM5. A niche object was created with the output "NeighborhoodToCell" and "ReceivingType" as identities, which were used for dimensional reduction with the following functions: FindVariableFeatures %>% ScaleData %>% RunPCA %>% RunUMAP. Overlapping spots or spots in close proximity within a reduced dimensional space were interpreted as an indicator of a shared microenvironment between the inflamed cell populations or cell types within these cell populations.

2.11 Differential gene expression and pathway analysis

Differential levels of gene expression between cell populations were assessed using the Seurat function "FindAllMarkers," with the parameters min.pct = 0.25, logfc.threshold = 0.5, and p val_adj < 0.01. Downstream analyses were performed on the upregulated DEGs. The top 10 genes with the highest expression levels within each cell population were defined as those with the highest average $\log_2$ fold change.

Pathway activity analyses were performed using the R package Progeny (version 3.19),[19] which uses an extensive collection of publicly accessible perturbation experiments to infer pathway activity. Heatmaps of pathway activity were generated from summarised progeny scores using the pheatmap R function and clustering_method = "median." Line plots were generated by transforming the summarised progeny scores into $\log_2$ fold change relative to the "noninflamed" biopsy region dataset as baseline.

Pathway enrichment analyses were performed using the R package cluster profiler[20] and gene expression markers from the inflamed cell populations as defined by differential gene expression analyses. The function "compareCluster" was used to identify biological processes common and specific to the inflamed cell populations using the following parameters: OrgDb = "org.Hs.eg.db," ont = "BP," keyType = "SYMBOL," fun = "enrichGO," pvalueCutoff = 0.01. Visualization of enrichment results were performed using the clusterprofiler function emapplot, which served as a guide to select groups of biological processes relevant to the inflamed cell populations.

2.12 Data illustration

Illustrations of UMAP plots, dot plots, and bar plots were achieved using the dittoseq R package (version 1.16.0).[21] Line plots were generated with ggplot2 R package (version 3.5.1).[22]

3. Results

3.1 Study population

This study utilized 43 biopsies collected at Weill Cornell Medical College from the colon ($n = 13$), ileum ($n = 15$), and anastomosis ($n = 15$) of 15 prospectively recruited patients with CD who had undergone prior ileocolonic resection (Figure 1) from the PREDICT-OR study.[23] Among the 15 patients (average age 39 years), there were 10 females, 4 former smokers, and 10 patients with endoscopic inflammation (Rutgeerts score ≥i2 or a Simplified Endoscopic Score for CD [SES-CD] score ≥3) in at least one biopsy location. Disease behaviors (Montreal classification) were nonstricturing, nonpenetrating (B1) (2 patients), stricturing (B2) (8 patients), and mixed stricturing and fistulizing (B2/B3) (5 patients). Disease locations were ileal (L1) (7 patients) and ileocolonic (L3) (8 patients). Therapies at the time of sample collection were biologics (10 patients), immunomodulators (2 patients), antibiotics (4 patients), and bile acid

sequestrants (4 patients). Summary tables of the number of samples defined by histologic and endoscopic assessments and by disease behavior and biologic use are found in Supplementary Information, Table S1.

3.2 Common transcriptomic pathway activity in inflamed biopsy regions from the colon, neo-terminal ileum, and anastomosis

Hierarchical clustering analyses of the transcriptional pathway activity in intestinal biopsies were performed and independently replicated using assessments based on endoscopy and histology. Findings at both levels were similar (Supplementary Information, Table S2). Compared to noninflamed counterparts, endoscopically inflamed (Figure 2A) and histologically active biopsy regions (Figure 2B) were marked by increased activity of the TNF-α, nuclear factor (NF)κB, Janus kinase/signal transducers and activators of transcription (JAK-STAT), epidermal growth factor receptor (EGFR), and mitogen-activated protein kinase (MAPK) signaling pathways. When using both endoscopic and histologic assessments in combination, histologic inflammation was the predominant determinant of pathway activity (Figure 2C). Biopsies were segregated into those with (1) histologically inflamed biopsy regions (irrespective of endoscopic inflammation status); and (2) biopsy regions that were not inflamed (ie, either without inflammation or adjacent to histologic inflammation). Histologically inflamed biopsy regions showed unique inflammatory pathway activity.

Histologically inflamed biopsy regions showed a conserved inflammatory signature across the colon, neo-terminal ileum, and anastomosis. This signature showed increased activity of the TNF-α, NFκB, JAK-STAT, EGFR, and MAPK pathways. The transcriptional profiles from inflamed biopsy regions were conserved across the 3 anatomic locations and were more similar to intersegmental inflamed biopsy regions than to intrasegmental biopsy regions that were not inflamed (Figure 2D). In contrast to the common intersegmental signature of inflamed biopsy regions, noninflamed biopsy regions differed from one another based on their anatomic location. Anastomotic biopsy samples exhibited transcriptional signatures that resembled the most represented segment, either ileum or colon (Figure 2E). Signal strength of transcriptional upregulation was greater in the inflamed colon or anastomosis than in the inflamed ileum (Figure 2D,E).

When analyses were stratified by anatomic location (ie, colon, neo-terminal ileum, and anastomosis), inflamed biopsy regions showed preserved transcriptional pathway activity across all anatomic locations (Figure 2F-I). Pathways that were strongly upregulated included the TNF-α, NFκB, JAK-STAT, EGFR, and MAPK pathways.

3.3 A common cellular composition in inflamed biopsy regions from the colon, neo-terminal ileum, and anastomosis

Dimensional reduction of all samples revealed that noninflamed cells segregated based on anatomic location, whereas inflamed cells segregated together irrespective of anatomic location (Figure 3A,B). Inflamed biopsy regions are composed mostly of T cells, B cells, and myeloid cells, whereas noninflamed biopsy regions are composed mostly of epithelial cells (Figure 3C).

A clustering analysis revealed the existence of 13 cell populations each representing a group of one or more cell types that share a similar transcriptomic profile. Cell populations were then classified by whether the majority of the cells were found upon histologically inflamed ("inflamed" cell populations) or noninflamed ("noninflamed" cell populations) biopsy regions (Figure 3D, Supplementary Information, Table S3). Cell composition in the inflamed cell populations was consistent across the 3 anatomic locations (Figure 4, Supplementary Information, Table S3). Specifically, cell type decomposition and cellular niche analysis revealed that immune cells (eg, myeloid, T cells, and B cells) and epithelial cells in close proximity shared a similar microenvironment in 3 inflamed cell populations, while the fourth cell population was composed of more than 90% epithelial cells. Differentially expressed genes (DEGs) from the inflamed cell populations were similarly expressed across intestinal anatomic locations including inflamed anastomotic biopsies and were enriched for signaling pathways involving immune cell recruitment/activation, inflammatory signaling, extracellular matrix (ECM) organization, and the oxidative stress response.

3.4 A common gene expression pattern across different inflamed cell types

The gene expression pattern of the top 10 upregulated DEGs from the inflamed cell populations was consistent with cellular identity and an inflammatory gene signature (Figure 5A, Supplementary Information, Table S4).

When segregating gene expression findings of inflamed biopsies by cell population, the strongest and most consistently upregulated genes were TNF-α, NF-κB, and JAK-STAT. In addition, clusters involving the specialized inflamed epithelial population had the strongest signal for these genes (Figure 5B, Supplementary Information Table S2).

Findings from pathway enrichment analysis performed with upregulated DEGs of inflamed cell populations were consistent with pathway activity and differential gene expression. (Supplementary Information, Figure S1, Table S5).

3.5 Different cell populations show gene expression associated with unique functions

Myeloid and mesenchymal cells from the inflamed T-cell/B-cell/myeloid population showed a gene expression pattern consistent with ECM remodeling and leukocyte recruitment (Supplementary Information, Figure S2). The inflamed B-cell/epithelial population presented a gene expression profile associated with the endoplasmic reticulum (ER) stress response (Supplementary Information, Figure S3). The inflamed epithelial and myeloid cell population was associated with a response to interferon-gamma (Supplementary Information, Figure S4). Lastly, the inflamed epithelial cell population showed expression patterns that were consistent with hypoxia, production of reactive oxygen species, and increased cellular metabolism (Supplementary Information, Figure S5).

3.6 Inflammatory activity and distribution according to biologic use

Inflammatory pathway activity (TNF-α, NFκB, JAK-STAT, and EGFR) was decreased in inflamed ileal biopsy regions from patients who were receiving biologics compared to those from patients who were not receiving biologics. However, representation of inflamed cell populations remained constant, regardless of biologic use (Supplementary Information, Figure S6). These subgroup data were limited due to sample size.

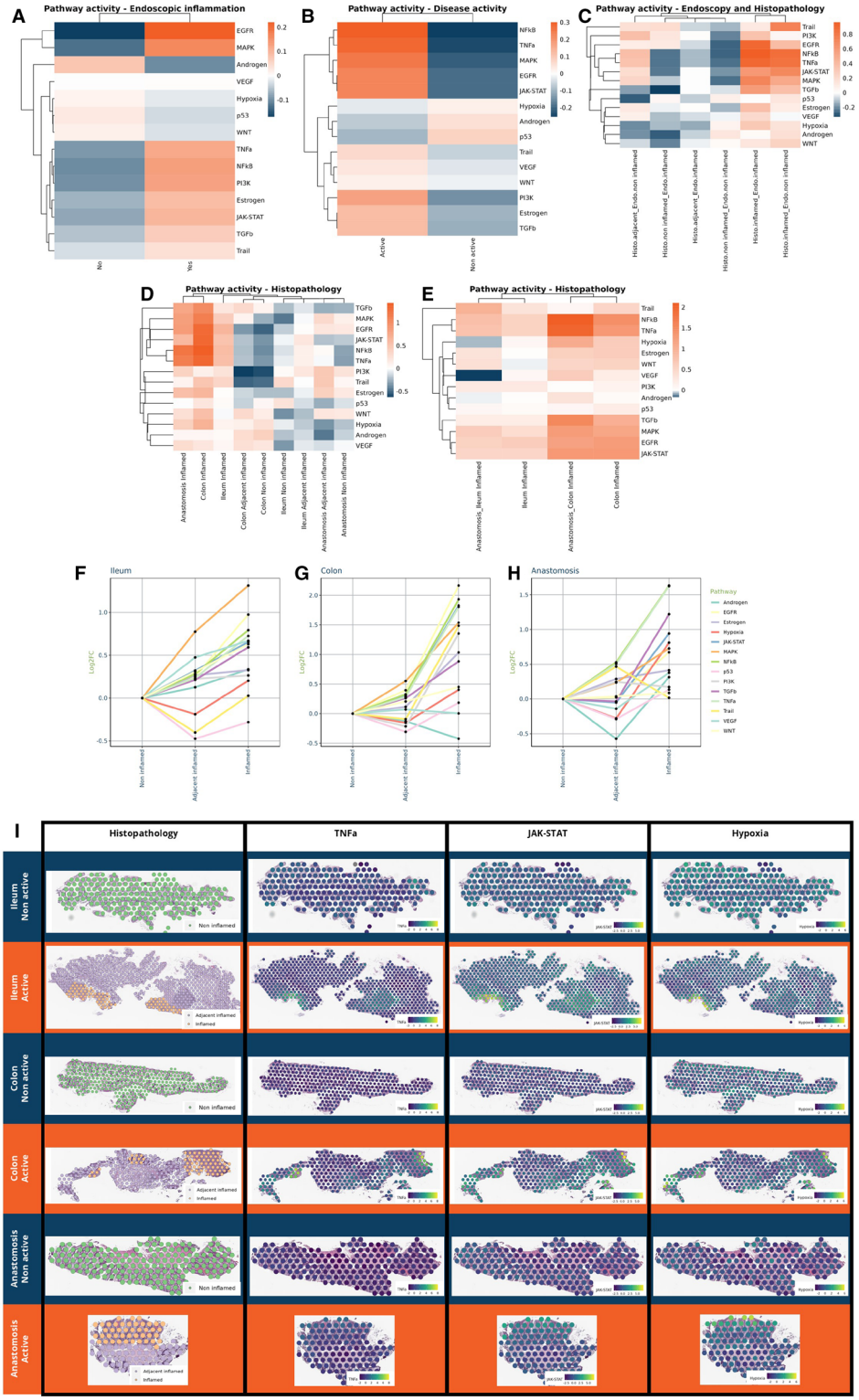


Figure 2. Pathway activity analyses correlated with endoscopic and histopathology assessments of colon, ileum, and anastomosis biopsies. (A) Hierarchical clustering of pathway activity profiles in samples defined by endoscopic inflammation (Yes = inflamed versus No = noninflamed). (B) Hierarchical clustering of pathway activity profiles in samples defined by histologic disease activity (nonactive disease vs. active disease). (C) Hierarchical clustering of pathway activity profiles in biopsy regions defined as inflamed or noninflamed by endoscopy (Endo.inflamed vs. Endo.non inflamed) and independently defined by histopathological annotations as inflamed, adjacent to inflamed, and noninflamed (inflamed: Histo.inflamed, adjacent-inflamed: Histo.adjacent, noninflamed: Histo.non inflamed), assessed in combination. (D) Pathway activity profiles in biopsy regions from the ileum, colon, and the anastomosis histologically defined as inflamed, adjacent-inflamed, and noninflamed. (E) Pathway activity profiles of histologically inflamed biopsy regions from the ileum, colon, and the anastomosis containing tissue from either ileum (anastomosis-ileum) or colon (anastomosis-colon). (F-H) Line plots displaying the fold change of pathway activity relative to noninflamed regions (histopathological assessment) in the ileum (F), colon (G) and the anastomosis (H). (I) Pathway activity spatial heatmaps of TNF-α, Janus kinase/signal transducers and activators of transcription (JAK-STAT), and hypoxia-associated transcriptional signatures in regions defined by histopathological assessments of colon, ileum, and the anastomosis samples.

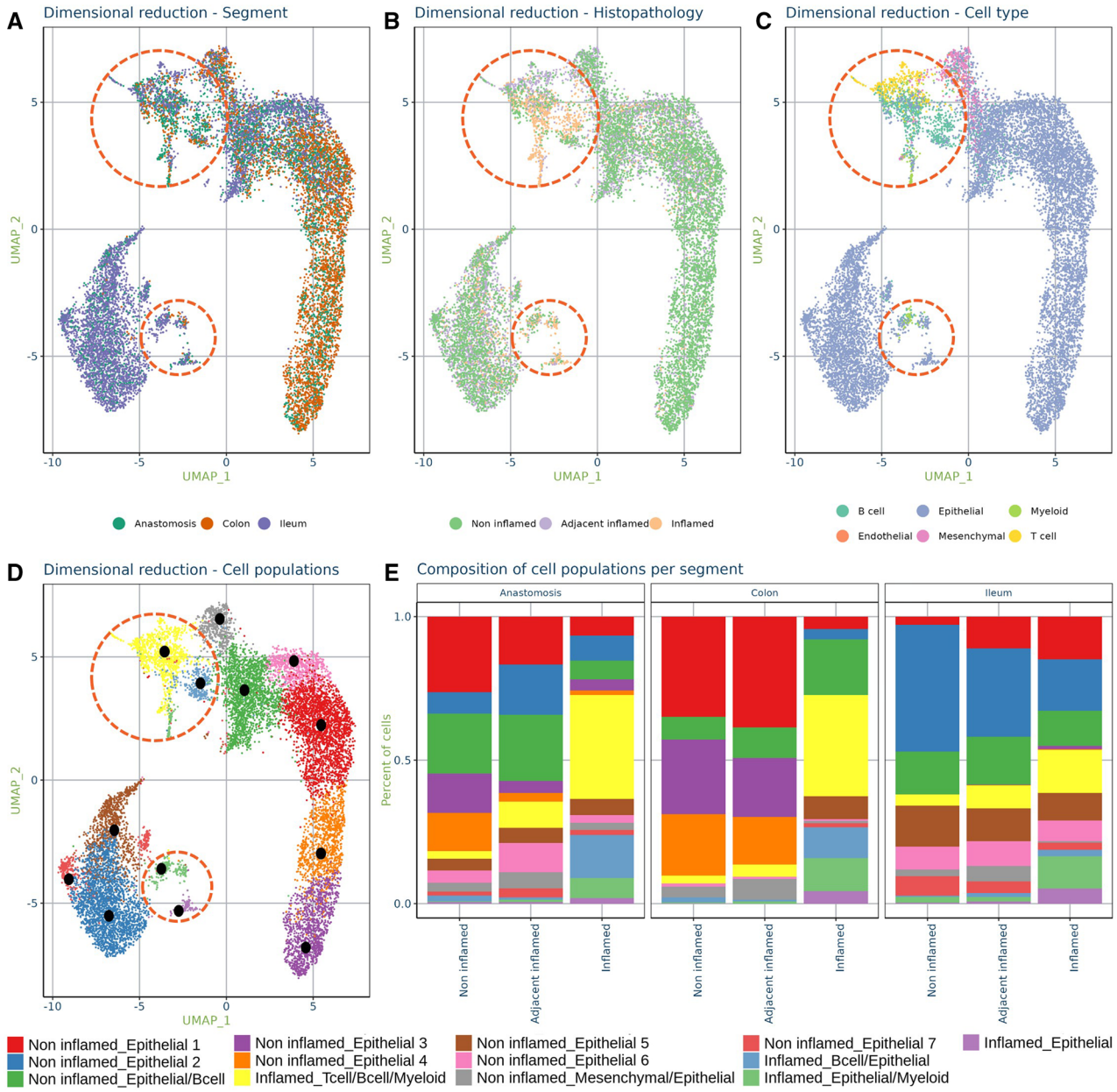


Figure 3. Dimensional reduction revealed cellular niches associated with histologic inflammation. (A-C) Uniform manifold approximation and projection (UMAP) plot of cells stratified by intestinal segment (colon, ileum, and anastomosis) (A), histopathology annotations (B), and cell type (C), highlighting (orange dashed circle) groups of cells from histologically inflamed and adjacent regions. (D) Uniform manifold approximation and projection (UMAP) plot of clustering results highlighting the inflamed cell populations (orange dashed circle). (E) Proportional contribution of cell types within cell populations in samples from the colon, ileum, and anastomosis.

4. Discussion

This study utilized spatial transcriptomics to reveal molecular signatures associated with inflammation in mucosal biopsies from patients with postoperative CD, leading to the identification of shared cellular niches and an epithelial cell type associated with regions of histologic inflammation across the colon, neo-terminal ileum, and the anastomosis. Pathway activity analyses of spatial transcriptomics indicated that histologic assessments of inflamed intestinal biopsy regions should be prioritized over endoscopic assessments.

Despite the distinct transcriptional signatures of noninflamed biopsy regions in the colon and ileum, the histologically inflamed biopsy regions of these anatomic locations and the anastomosis shared transcriptional signatures across 3 cellular niches and an epithelial cell type defined by enhanced expression of inflammation-associated genes. Identification of these inflamed cell populations prompted further characterization of gene expression, cell-type composition, and cellular roles in the inflammatory process. In postoperative CD, inflamed biopsy regions from all 3 anatomic locations demonstrated a similarly increased abundance of immune cells and inflammatory gene expression patterns as opposed to hypoxic pathways. In addition to TNF-α and JAK-STAT gene expression pathways that are targeted by current treatments, EGFR and MAPK pathways were also identified in this study.

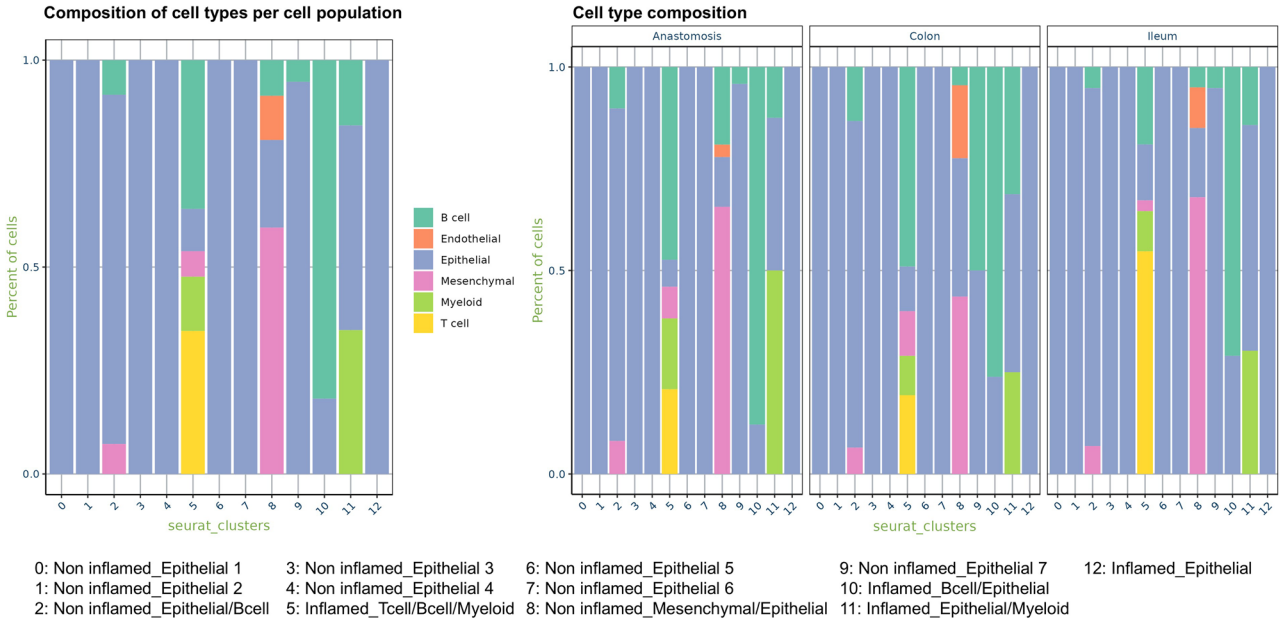


Figure 4. Cell type composition. Cell type composition per cell population for all segments combined (A) and for the data stratified by segment (B).

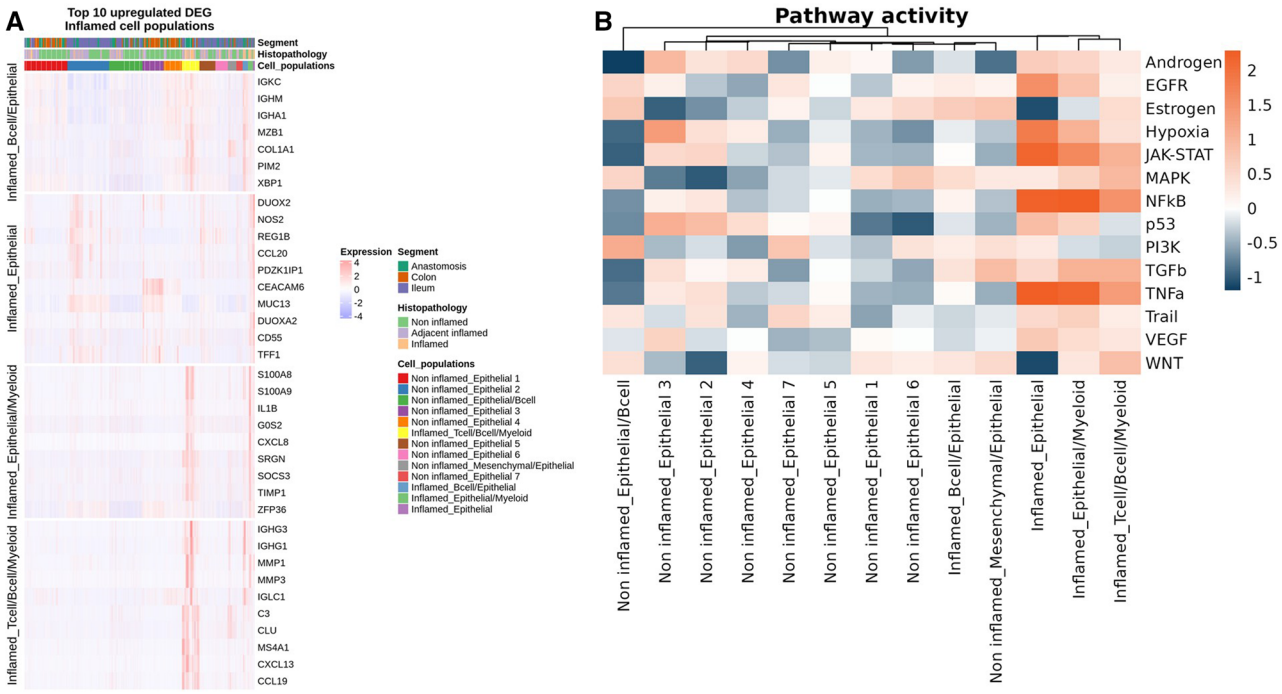


Figure 5. Differential gene expression, pathway activity, and pathway enrichment analysis. (A) Heatmap illustrating the expression of the top 10 upregulated differentially expressed genes (DEGs) (inflamed B-cell/epithelial and inflamed epithelial/myeloid share top 10 upregulated DEGs with the remaining inflamed cell populations and less than 10 genes are displayed) in the inflamed cell populations, in the entire dataset stratified by intestinal segment, histopathology annotations, and cell populations. (B) Hierarchical clustering of pathway activity profiles in the cell populations.

This study sheds light on the underlying pathophysiology of the commonly encountered clinical scenario of anastomotic ulceration and variations of postoperative CD recurrence. For patients with ulceration in the colon, ileum, or at the anastomosis, the data collectively show that this ulceration represents CD recurrence as opposed to ischemia, which may guide appropriate management decisions. While specific management of ulceration in the postoperative context requires further study, data have shown that the elimination of CD-related endoscopic ulceration is associated with better outcomes and should be the target of management.[24]

In addition to the underlying pathophysiological findings in postoperative CD, this study revealed the gene expression pattens associated with specific cells and functions that may identify therapeutic targets in this population. Specific functions included myeloid and mesenchymal cells involved in ECM remodeling and leukocyte recruitment, B-cell activation involved in the ER stress response, and granulocytes from the epithelial and myeloid

populations associated with a response to interferon-gamma. Lastly, the gene expression patterns of the unique inflamed epithelial cell population were more consistent than those of the other cell populations with hypoxia and increased cellular metabolism.

Uniquely, we have now characterized the presence of an inflamed epithelial cell population in postoperative CD. The cells in this population displayed similarities in spatial location and gene expression to the CD-associated "LND" cells recently discovered by Li et al. These cells have high expression of *LCN2*, *NOS2*, and *DUOX2*, and have been identified in inflamed colonic and ileal segments in CD.[25] Our findings provide independent validation of findings by Li et al. and identified the presence of these cells in the ileocolonic anastomosis.[25] The inflamed epithelial cell population is generated by a successful transformation of epithelial cells from the inflamed and noninflamed cell populations, which parallels increased reactive oxygen species, glycolysis, and lipid transport/metabolism gene expression from the progenitor inflamed epithelial/myeloid cell population. Further analysis of the inflamed epithelial cell population suggested that the synthesis and transport of type L apolipoproteins is a previously unrecognized role of lipid metabolism in IBD pathophysiology. There is a paucity of literature about the role of type L apolipoproteins in inflammation, and to our knowledge, no studies have correlated this group of apolipoproteins to IBD.

This study has some relevant strengths, including its delineation of the molecular mechanisms in postoperative CD and its identification of common transcriptomic pathway activity and a common cellular composition in inflamed biopsy regions from the colon, neo-terminal ileum, and anastomosis. In addition, this study found a common inflammatory gene expression pattern across different inflamed cell types when analyzing the most upregulated DEGs, while each inflamed cell population showed gene expression associated with a unique function. Spatial transcriptomic analyses revealed granular transcriptomic signatures through stratification of gene expression patterns by cell populations and spatial location. Limitations of this study are its cross-sectional nature and the sample sizes for subgroup evaluations of disease behavior and specific therapies.

In conclusion, understanding spatial context is important for unravelling the molecular mechanisms underlying CD. By identifying and characterizing cellular niches associated with histologically inflamed biopsy regions across the colon, neo-terminal ileum, and anastomosis, we provided granular insights into the drivers of inflammation stratified by spatial locations and cell populations in postoperative CD. Our work highlights the potential for using spatial transcriptomics to characterize inflammation-promoting cell populations and signaling pathways as novel treatment targets and biomarkers in CD.

Acknowledgments

Medical writing support was provided by David O'Gorman, PhD, a former employee of Alimentiv Inc, and Stefanie McFarlane, CMPP, an employee of Alimentiv Inc. Project management support was provided by Dax Torti, PhD, a former employee of Alimentiv Inc.

Author contributions

Robert Battat (Conceptualization [equal], Investigation [lead], Resources [equal], Writing—original draft [equal], Writing—review and editing [lead]), Bruno Sangiorgi (Conceptualization [equal], Methodology [lead], Formal analysis [lead], Writing—original draft [lead], Writing—review and editing [equal]), Bryan Linggi (Investigation [equal], Writing—review and editing [equal]), Xianyong Gui (Investigation [equal], Writing—review and editing [equal]), Michelle I. Smith (Project administration [lead], Writing—review and editing [equal]), Saurabh Mehandru (Investigation [equal], Writing – review and editing [equal]), Randy Longman (Supervision [equal], Resources [equal], Writing—review and editing [equal]), Dana J. Lukin (Resources [equal], Writing—review and editing [equal]), Ellen J. Scherl (Resources [equal], Writing—review and editing [equal]), Lihui Qin (Resources [equal], Writing—review and editing [equal]), Christopher Ma (Supervision [equal], Writing—review and editing [equal]), Wendy Teft (Conceptualization [equal], Supervision [equal], Writing—review and editing [equal]), and Niels Vande Casteele (Conceptualization [equal], Supervision [equal, Writing—review and editing [equal])

Supplementary material

Supplementary material is available at *ECCO-JCC* online.

Funding

None declared.

Conflicts of interest

R.B. reports speaker/consulting/moderator fees from Bristol Myers Squibb, Johnson and Johnson, AbbVie, Takeda, Ferring, Celltrion, Pfizer, and Pendopharm; advisory board fees from Celltrion, AbbVie, Pfizer, Lilly, Johnson and Johnson, Bristol Myers Squibb, Takeda, and Merck; and educational grants from Johnson and Johnson, AbbVie, Celltrion, Pfizer, Pendopharm, Amgen, Organon, Merck, and Eli Lilly. B.S., M.I.S., and W.T. are employees of Alimentiv Inc. B.L. is a former employee of Alimentiv Inc. X.G. and N.V.C. are former employees of AcelaBio Inc. S.M. reports receiving research grants from Genentech, Bristol Myers Squibb (BMS), and Takeda; reports receiving payment for lectures from Takeda, Genentech, and Morphic; and reports receiving consulting fees from Takeda, Morphic, BMS, Ferring, and Arena Pharmaceuticals. R.L. has received consulting fees from Pfizer and Roivant and research support from Boehringer Ingelheim. D.J.L. reports consulting for AbbVie, Boehringer Ingelheim, BMS, Eli Lilly, Fresenius Kabi, Janssen, PSI, Palatin Technologies, Pfizer, Prometheus Laboratories, and Takeda; has received grants from AbbVie, Boehringer Ingelheim, Crohn's & Colitis Foundation, Janssen, and Takeda; and has received speaking fees from AbbVie and Janssen. E.J.S. reports receiving grant/research support from Abbott (AbbVie), AstraZeneca, CCFA, Janssen Research & Development, Johns Hopkins University, National Institute of Diabetes and Digestive and Kidney (NIDDK), National Institute of Health (NIH), New York Crohn's Foundation, Pfizer, UCB, UCSF–CCFA Clinical Research Alliance, Genentech, Seres Therapeutics, and Celgene Corporation; reports serving as Consultant/Advisory Board for AbbVie, Crohn's and Colitis Foundation of America (CCFA), Entera Health, Evidera, GI Health Foundation, Janssen, Protagonist Therapeutics, Seres Health, Takeda Pharmaceuticals, and Bristol Myers Squibb; is a Gilead stock shareholder; and has received honoraria from

GI Health Foundation and Janssen for nonbranded speaker's bureau. L.Q. reports no conflicts of interest. C.M. has received consulting fees from AbbVie, Alimentiv, Amgen, AVIR Pharma, Bristol Myers Squibb, Ferring, Fresenius Kabi, Janssen, McKesson, Mylan, Takeda, Pfizer, and Roche; speaker's fees from AbbVie, Amgen, AVIR Pharma Inc, Alimentiv, Ferring, Janssen, Takeda, and Pfizer; and research support from Pfizer. Alimentiv Inc. is an academic gastrointestinal contract research organization (CRO), operating under the Alimentiv Health Trust. Alimentiv Inc. provides comprehensive clinical trial services, precision medicine offerings, and centralized imaging solutions for endoscopy, histopathology, and other imaging modalities. The beneficiaries of the Alimentiv Health Trust are the employees of the enterprises it holds. CM is a consultant to Alimentiv Inc. and has a primary academic appointment; he does not hold equity positions or shares in Alimentiv Inc.

Data availability

All data relevant to the study are included in the article or uploaded as supplementary files.

Ethics statement

The biopsies used in the current study were from a previous study that was approved by the Weill Cornell Medical College (WCMC) Institutional Review Board (#00009417, #00009419; ID 19-09020855). All patients provided prior consent to participate in the study.

References

1. Rutgeerts P, Geboes K, Vantrappen G, et al. Predictability of the postoperative course of Crohn's disease. *Gastroenterology*. 1990;99:956-963.
2. Dulai PS, Levesque BG, Feagan BG, D'Haens G, Sandborn WJ. Assessment of mucosal healing in inflammatory bowel disease: review. *Gastrointest Endosc*. 2015;82:246-255.
3. Shah SC, Colombel JF, Sands BE, Narula N. Systematic review with meta-analysis: mucosal healing is associated with improved long-term outcomes in Crohn's disease. *Aliment Pharmacol Ther*. 2016;43:317-333.
4. Khanna R, Bressler B, Levesque BG, et al. Early combined immunosuppression for the management of Crohn's disease (REACT): a cluster randomised controlled trial. *Lancet*. 2015;386:1825-1834.
5. Tsai L, Ma C, Dulai PS, et al. Contemporary risk of surgery in patients with ulcerative colitis and Crohn's disease: a meta-analysis of population-based cohorts. *Clin Gastroenterol Hepatol*. 2021;19:2031-2045.e11.
6. Luglio G, Pellegrini L, Rispo A, et al. Post-operative morbidity in Crohn's disease: what is the impact of patient-, disease- and surgery-related factors? *Int J Colorectal Dis*. 2022;37:411-419.
7. Hirten RP, Mashiana S, Cohen BL, et al. Ileocolic anastomotic inflammation after resection for Crohn's disease indicates disease recurrence: a histopathologic study. *Scand J Gastroenterol*. 2020; 55:795-799.
8. Hammoudi N, Auzolle C, Tran Minh ML, et al. Postoperative endoscopic recurrence on the neoterminal ileum but not on the anastomosis is mainly driving long-term outcomes in Crohn's disease. *Am J Gastroenterol*. 2020;115:1084-1093.
9. Martin JC, Chang C, Boschetti G, et al. Single-cell analysis of Crohn's disease lesions identifies a pathogenic cellular module associated with resistance to anti-TNF therapy. *Cell*. 2019;178: 1493-1508.e20.
10. Guilliams M, Bonnardel J, Haest B, et al. Spatial proteogenomics reveals distinct and evolutionarily conserved hepatic macrophage niches. *Cell*. 2022;185:379-396.e38.
11. Pai RK, Khanna R, D'Haens GR, et al. Definitions of response and remission for the Robarts Histopathology Index. *Gut*. 2019; 68:2101-2102.
12. Hao Y, Hao S, Andersen-Nissen E, et al. Integrated analysis of multimodal single-cell data. *Cell*. 2021;184:3573-3587.e29.
13. Korsunsky I, Millard N, Fan J, et al. Fast, sensitive and accurate integration of single-cell data with Harmony. *Nat Methods*. 2019;16:1289-1296.
14. Street K, Risso D, Fletcher RB, et al. Slingshot: cell lineage and pseudotime inference for single-cell transcriptomics. *BMC Genomics*. 2018;19:477.
15. Cable DM, Murray E, Zou LS, et al. Robust decomposition of cell type mixtures in spatial transcriptomics. *Nat Biotechnol*. 2022;40:517-526.
16. Elmentaite R, Kumasaka N, Roberts K, et al. Cells of the human intestinal tract mapped across space and time. *Nature*. 2021; 597:250-255.
17. Raredon MSB, Yang J, Kothapalli N, et al. Comprehensive visualization of cell-cell interactions in single-cell and spatial transcriptomics with NICHES. *Bioinformatics*. 2023;39:btac775.
18. Linderman GC, Zhao J, Roulis M, et al. Zero-preserving imputation of single-cell RNA-seq data. *Nat Commun*. 2022;13:192.
19. Schubert M, Klinger B, Klunemann M, et al. Perturbation-response genes reveal signaling footprints in cancer gene expression. *Nat Commun*. 2018;9:20.
20. Wu T, Hu E, Xu S, et al. clusterProfiler 4.0: a universal enrichment tool for interpreting omics data. *Innovation (Camb)*. 2021;2: 100141.
21. Bunis DG, Andrews J, Fragiadakis GK, Burt TD, Sirota M. dittoSeq: universal user-friendly single-cell and bulk RNA sequencing visualization toolkit. *Bioinformatics*. 2021;36:5535-5536.
22. Wickham H. *ggplot2: Elegant Graphics for Data Analysis*. Springer-Verlag; 2016.
23. *PhaRmacokinEtic and pharmacoDynamics of Therapies, non-Inflammatory Surgical Complications and predicTive Biomarkers in pOst-opeRative Crohn's Disease (PREDICT-OR) study*. Weill Cornell Medicine; 2022.
24. Turner D, Ricciuto A, Lewis A, et al. STRIDE-II: an update on the selecting therapeutic targets in inflammatory bowel disease (STRIDE) initiative of the International Organization for the Study of IBD (IOIBD): determining therapeutic goals for treat-to-target strategies in IBD. *Gastroenterology*. 2021;160:1570-1583.
25. Li J, Simmons AJ, Hawkins CV, et al. Identification and multimodal characterization of a specialized epithelial cell type associated with Crohn's disease. *Nat Commun*. 2024;15:7204.